5th International Conference on Silicon Photovoltaics, SiliconPV 2015

The influence of ITO dopant density on J-V characteristics of silicon heterojunction solar cells: experiments and simulations

Simon Kirner[a], Manuel Hartig[b], Luana Mazzarella[a], Lars Korte[c], Tim Frijnts[a], Harald Scherg-Kurmes[b], Sven Ring[a], Bernd Stannowski[a], Bernd Rech[c], Rutger Schlatmann[a]

[a]PVcomB, Helmholtz-Zentrum Berlin für Materialien und Energie, Schwarzschildstr. 3, 12489 Berlin, Germany
[b] Technische Universität Berlin, Fakultät IV, HFT 5-2, Einsteinufer 25, 10587 Berlin, Germany
[c] Institut für Silizium Photovoltaik, Helmholtz-Zentrum Berlin für Materialien und Energie
Kekuléstraße 5, 12489 Berlin, Germany

Abstract

The TCO/a-Si:H(p) contact is a critical part of the silicon heterojunction solar cell. At this point, holes from the emitter have to recombine loss free with electrons from the TCO. Since tunneling is believed to be the dominant transport mechanism, a high dopant density in both adjacent layers is critical. In contrast to this, it has been reported that high TCO dopant density can reduce field effect passivation induced by the a-Si:H(p) layer. Thus, in this publication, we systematically investigate the influence of a thin (~10 nm) ITO contact layer with dopant densities ranging from $N_d = 10^{19} - 10^{21}$ cm^{-3} placed between an ITO bulk layer of 70 nm with $N_d = 2\cdot10^{20}$ cm^{-3} and the a-Si:H(p) emitter on the J-V characteristics, with the aim to find an optimum N_d. We accompanied our experiments by *AFORS-HET* simulations, considering trap-assisted tunneling and field dependent mobilities in the a-Si:H(p) layer. As expected, two regimes are visible: For low N_d the devices are limited by inefficient tunneling, resulting in S-shaped J-V characteristics. For high N_d a reduction of the field effect passivation becomes visible in the low injection range. We can qualitatively reproduce these findings using device simulations.

Keywords: Silicon hetero junction solar cells, HIT, TCO/a-Si:H(p) contact, ITO, tunneling, AFORS-HET,

1. Introduction

Silicon heterojunction (*SHJ*) solar cells consisting typically of a stack of transparent conducting oxide (*TCO*)/a-Si:H(p/i)/c-Si(n) wafer/a-Si:H(i/n)/*TCO*/metal are well known for their very high conversion efficiency [1]. The key advantage of this solar cell type is that there is no direct contact between the metal contacts and the absorber. Instead, the full area of the wafer surfaces is passivated by high quality a-Si:H(i) passivation layers allowing very

low surface recombination velocities. This however makes contacting of the solar cell challenging. Especially the emitter contact, consisting of a TCO, often indium tin oxide (ITO), deposited on the a-Si:H(p) emitter usually induces a considerable contact resistance [2]. Several studies have addressed this issue theoretically by means of device simulation. For example, Centurioni *et al.* have calculated using the device simulator *AMPS* that starting from a TCO work function of ϕ_{ITO} = 5.1 eV, a change by -350 meV could reduce the energy conversion efficiency, η, of the device by more than 40% due to the formation of an S-shaped current-voltage-(J-V-)characteristic. These findings were ascribed to the formation of a rectifying contact at the ITO/a-Si:H(p) interface. A further reduction to ϕ_{ITO} = 4.3 eV lead to a complete blocking behavior of the cell. Similar results were calculated by Varache *et al.* [3] and Zhao *et al.* [4] using *AFORS-HET*, by Rached *et al.* using Amorphous Semiconductor Device Modeling Program [5] and Bivour *et al.* (*AFORS-HET*) [6]. All of these studies predict a high η only for ϕ_{TCO} > 4.8 eV. Then, ϕ_{TCO} approaches the value of $\phi_{a-Si:H(p)}$ ~ 5.2 eV, which can be calculated within the Anderson model to $\phi_{a-Si:H(p)} = X_{a-Si:H(p)} + E_{g,\,a-Si:H(p)} - E_{act,\,a-Si:H(p)}$, with X being the electron affinity, E_g the mobility gap and E_{act} the activation energy (distance between Fermi-level and valence band), cf. Fig. 1c. If the Anderson model is valid, the band offset, $\Delta\phi$, becomes zero, when $\phi_{TCO} = \phi_{a-Si:H(p)}$. In this case or when the work function difference is sufficiently low, transport across the junction via thermionic emission is efficient enough, corresponding to a loss free contact. If $\Delta\phi$ is high, tunneling is required for a loss free contact [7]. For an efficient tunnel contact, it is essential for *both* adjacent layers to be highly doped. Under the assumption of a constant X_{TCO}, this means a low ϕ_{TCO} is desirable for an efficient tunnel contact. This aspect is only visible, if the TCO is calculated as a semi-conductor, as opposed to a metal as it has been treated in the above mentioned references [2–6]. In Fig.1b and c, the difference between the two approaches can be seen: If the TCO is treated as a metal, an increase in ϕ_{TCO} leads only to a decrease in band bending on the a-Si:H(p) side, the negative effect on the TCO side is neglected. On the other hand, if the TCO is treated as a semi-conductor, an increase in ϕ_{TCO} leads also to a band bending on the TCO side. This aspect has not been discussed in much detail in literature so far.

Another aspect that has to be considered in this context is the interplay between TCO doping and absorber passivation. It has recently been shown that the deposition of a highly doped TCO can reduce the effective life time due to a reduction of the field effect passivation at the a-Si:H/c-Si interface, which is clearly visible in injection level dependent measurements such as photo-conductance decay- or illumination dependent open-circuit voltage (Suns-V_{oc}) measurements [8,9]. This reduced field effect passivation can lead to a fill factor deterioration. This again speaks for a low $N_{d,\,TCO}$ (high ϕ_{TCO}) as being beneficial for the device performance.

As reported in literature, the work function of ITO, ϕ_{ITO}, can be manipulated via the deposition parameters over the dopant concentration N_d $\phi_{a-Si:H(p)}$: e.g. Klein et al. show data between ~4.2 – 5.3 eV. A convenient way to manipulate N_d is via the oxygen partial pressure during the deposition [10]. Further reported methods to manipulate ϕ_{ITO} are pre- and post-deposition treatments [11,12].
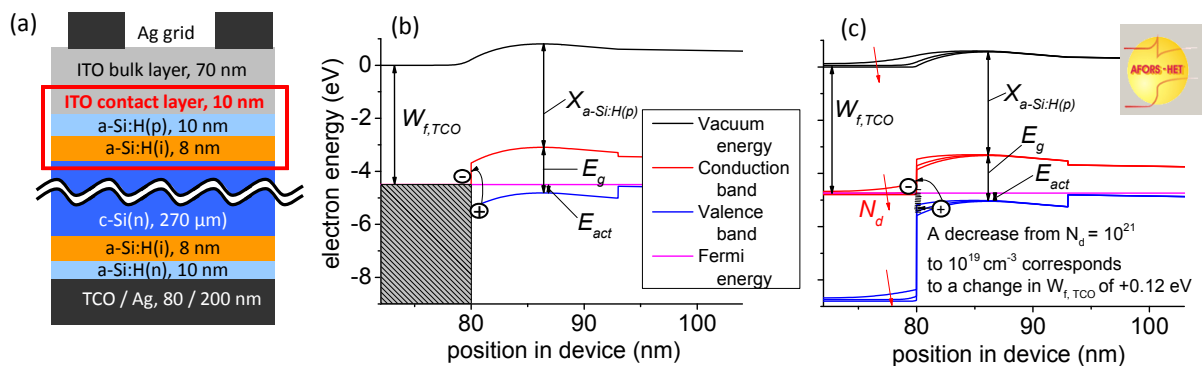

Fig. 1. (a) Device structure considered in this paper with the red box indicating the studied interface; (b) the respective band diagram zoomed-in to the TCO/a-Si:H(p) contact in case the TCO is treated as a metal or (c) treated as a semi-conductor for different dopant densities, N_d and corresponding work functions W_f of the TCO contact layer.

In this work, we use ITO with N_d ranging from $\sim 1\cdot 10^{19} - 1\cdot 10^{21}$ cm^{-3} as a 10 nm thin contact layer placed in between the a-Si:H(p) emitter and an ITO bulk layer (70 nm, $N_d = 2\cdot 10^{20}$ cm^{-3}) of *SHJ* solar cells. We observed that solar cells with contact layers with $N_d < 2\cdot 10^{19}$ cm^{-3} show a considerable decrease in *FF*. On the other hand, pseudo *FFs* above 81% could still be measured with $N_d \sim 1\cdot 10^{21}$ cm^{-3}. The experimental results can be qualitatively reproduced using the device simulator *AFORS-HET* when certain tunneling related models are considered. This indicates that there is a trade-off between field effect passivation and a low resistivity tunnel contact when considering the optimal N_d.

2. Experimental methods

ITO films have been deposited by means of DC magnetron sputtering in a Leybold Optics system designed for substrate sizes of up to 30×30 cm² at a heater temperature of 220°C. The contact layer was deposited at $6.7\cdot 10^{-6}$ bar and deposition power of 0.5 kW; the bulk layer was deposited with $3.6\cdot 10^{-6}$ bar and 1.0 kW. The total Ar- and mixed gas flow (10% O$_2$ in Ar) was 500 sccm and 250 sccm for the contact- and bulk-layer, respectively. The O$_2$ partial pressure in the contact layer was varied between 0.0 – 6.0%, which resulted in films with carrier densities of N_d ranging from $1\cdot 10^{19} - 1\cdot 10^{21}$ cm^{-3} as obtained from Hall measurements on ITO/glass samples with ITO-thicknesses ranging from 160 – 220 nm (results shown in Fig. 2). The bulk ITO layer was deposited with a constant O$_2$ partial pressure of 2.5% resulting in $N_d = 2\cdot 10^{20}$ cm^{-3}. Spectrophotometry measurements (not shown) revealed the expected increase in free carrier absorption in the near infra-red region of the spectrum with increasing N_d.
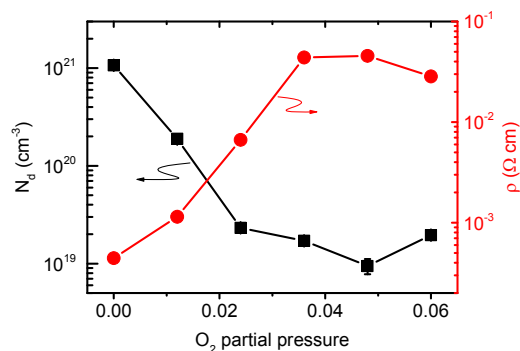

Fig. 2. ITO dopant density N_d and resistivity ρ as obtained from Hall measurements as a function of O$_2$ partial pressure. Film thickness was between 160-220 nm.

The solar cells were fabricated on c-Si(n) wafers (FZ, ~ 3 Ωcm resistivity, <111> termination, 270 µm thickness). Shiny etched wafer pieces were used to increase sensitivity to the contact resistivity. The layer stack is shown in Fig. 1a. Plasma enhanced chemical vapor deposition has been performed using an AKT-1600 tool to deposit the a-Si:H i/n and i/p stacks. A lowly, trimethylboron-doped a-Si:H(p) layer has been used as emitter [13]. The back contact consists of a ZnO:Al/Ag stack. The front TCO consists of the mentioned ITO contact- (10 nm) and bulk-layer (70 nm) stack. A Ti/Ag grid with thicknesses of 10 and 1500 nm has been deposited on top of the front TCO. Multiple cells per wafer were defined by means of photolithography with an area of 1 cm².

The devices were characterized by light J-V measurements using a sun simulator with dual-source illumination under standard test conditions (25°C, class AAA spectrum) and illumination dependent open-circuit voltage (Suns-V_{oc}) measurements. Measurements were performed through an aperture of 1 cm². The reported η and current density, J, values are calculated based on the aperture area (including the grid). Transmission-line-method-(*TLM-*)measurements were performed to test the influence of N_d in the contact layer on the sheet resistance, R_{sheet}, of the ITO layer stack on selected samples with dedicated test structures deposited on the same wafer as the solar cells.

3. *AFORS-HET* model and tunneling models

A general description of the used simulation tool *AFORS-HET* can be found in Ref. [14]. The calculated layer stack consists of TCO/a-Si:H(p/i)/c-Si(n)/a-Si:H(i/n). For all of the layers except the TCO, *AFORS-HET* text book structures were used[*]. The data for the TCO and the a-Si:H(p) layer are given in the appendix. The surface recombination velocities at both contacts has been set to $1 \cdot 10^7$ cm/s to impose no additional loss mechanism.

To simulate tunneling at the TCO/a-Si:H(p) interface, two additional models have been used: the trap assisted tunneling (TAT) model based on the theory of Hurkx *et al.* [15] as well as the field-dependence of the mobilities (FDM) suggested by Willemen *et al.* [16,17]. TAT allows holes to tunnel into states in the band gap and thus the effective tunneling mass, m^*, has to be considered as a fraction of the electron mass, m^*. FDM is based on the finding that the mobility of a-Si:H increases exponentially under very high fields and a field constant F_0 has to be considered [18]. Both models depend heavily on the magnitude of the electric field, thus, have a very high sensitivity on the dopant densities in the adjacent layers. For m^* and F_o values from literature were taken [16,17]. In Fig. 3, the influence of the models on the J-V characteristics is shown. As can be seen, by considering both models, the blocking J-V characteristic of the device, induced by the *n/p/n* structure is avoided by making the TCO/a-Si:H(p) junction ohmic. A weakness of our approach is the fact that we assume Maxwell-Boltzmann- as opposed to Fermi-Dirac-statistics to calculate electron- and hole-densities in the TCO based on the density of states. This could theoretically lead to unrealistically high numbers. However, by carefully initializing the numerical model, we can confirm realistic electron densities close to N_d in the whole TCO (cf. Fig. 1c). Implementation of Fermi-Dirac statistics into *AFORS-HET* is ongoing. We expect a small difference in quasi Fermi level position, which would lead to minor differences when calculating an ideal N_d, but would not affect the general trend discussed in this paper.
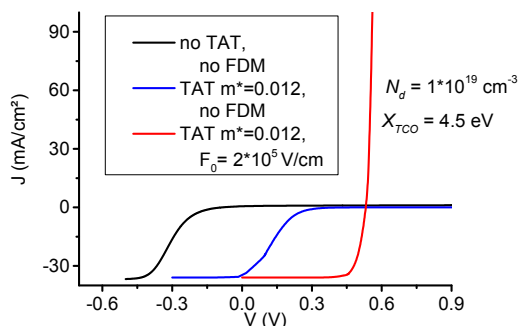

Fig. 3. Simulated J-V characteristics with and without the tunneling models TAT and FDM applied in the a-Si:H(p) emitter.

4. Results & discussion

4.1. Experimental results

The solar cell characteristics short-circuit current density, J_{sc}, fill factor, FF, open-circuit voltage, V_{oc} and power conversion efficiency, η, are shown in Fig. 4 as a function of N_d in the ITO contact layer. Also given are the differential resistances, R_{sc}, calculated from the inverse of the light J-V slope near short circuit conditions and R_{oc} calculated analogously near open circuit conditions. In the graph showing the FF, also the pseudo-FF data as obtained from Suns-V_{oc} measurements is shown for comparison. The following observations can be made: J_{sc} shows

---

[*] to be found online: http://www.helmholtz-berlin.de/forschung/oe/ee/si-pv/projekte/asicsi/afors-het/index_en.html

no systematic trend, some scattering is presumably related to a process error leading to increased under-evaporation during grid deposition for some samples. Increase in parasitic absorption due to increased free carrier absorption for very high N_d is believed to play only a minor role given the low contact layer thickness. The *FF* is overall on a relatively low level. We explain the large discrepancy to the pseudo *FF* by the low doping of the a-Si:H(p) layer and the resulting losses at the TCO/a-Si:H(p) contact. With respect to the influence of N_d, one can observe an increase for contact layers up to $>2 \cdot 10^{19}$ cm^{-3}. Above this value, the trend is ambiguous due to the small number of data points but a small decrease in *FF* and pseudo *FF* is apparent. When looking at R_{oc}, R_{sc} and the shape of the curve at high forward bias shown in Fig. 5a, one can observe that the reduction in FF is due to a more pronounced S-shape of the J-V curve. This, as we show below in more detail, can be explained by increasingly inefficient tunneling though the increasing space charge region at the TCO/a-Si:H(p) interface (Schottky-diode as opposed to ohmic behavior of the TCO/a-Si:H(p) junction) [19]. The small observable decrease in *FF* for very high N_d is accompanied by a pronounced reduction in effective carrier lifetime for low minority carrier densities, as obtained from SunsV$_{oc}$ measurements and shown in Fig. 5b. This can be explained by the reduction of field effect passivation, which usually affects more the *FF* than the V_{oc} due to the shape of the lifetime versus minority carrier density curves [8]. The latter is therefore, as expected, relatively unaffected by the change in N_d and thus η follows mainly the trend of the *FF*.

To confirm that the decrease in *FF* is predominantly related to the contact resistance, the sheet resistance of the ITO contact and bulk layer stack has been measured on the *TLM* structures on the samples with $N_d = 1.9 \cdot 10^{19}$ cm^{-3} (average *FF* = 68%) and $N_d = 2.3 \cdot 10^{19}$ cm^{-3} (average *FF* = 71%). It increased by only <5 Ω$_\square$. Given the geometry of the metal grid, this would lead to an expected increase in series resistance of < 0.02 Ωcm^2, which can hardly explain the drop in *FF*. This and the pronounced S-shaped J-V characteristics are strong indications that insufficient tunneling at the TCO/ a-Si:H(p) interface is the dominating mechanism reducing the *FF*.
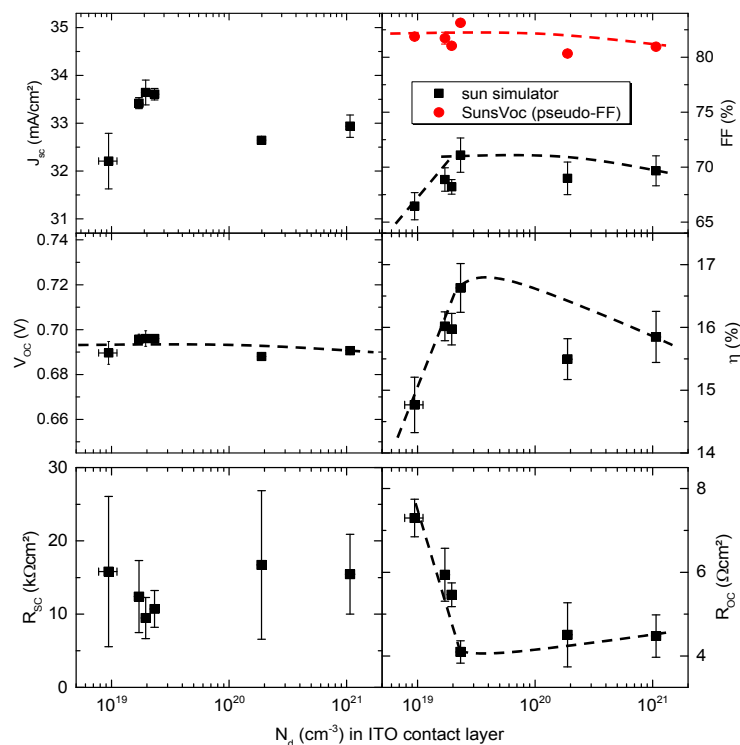

Fig. 4. Solar cell characteristics as obtained from light J-V- and Suns-V$_{oc}$-measurements as a function of the dopant density, N_d in the ITO contact layer. Lines are guides to the eye indicating the influence of N_d on the two mechanisms: Tunneling and field effect passivation.
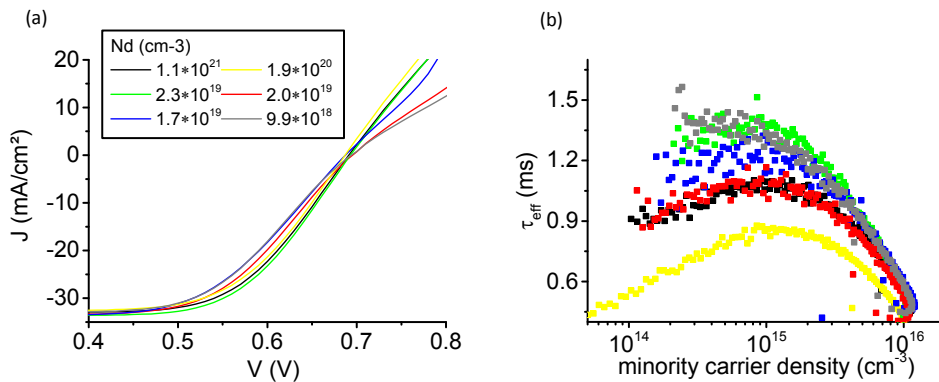
Fig. 5. (a) Experimentally obtained light J-V characteristics under high forward bias and (b) effective carrier densities as a function of minority carrier density for selected cells with different N_d. The color code is the same for both graphs.

4.2. Simulation results

Variations of the dopant density, N_d, in the TCO of the above described model structure have been performed and for two different electron affinities X_{TCO} and the light J-V characteristics have been calculated. The results are shown in Fig. 6. Simulations show qualitatively similar trends as the experiments: J-V curves of structures with low N_d become S-shaped due to insufficient tunneling at the TCO/a-Si:H(p) interface. There is only a small reduction of V_{oc} visible, which could be related to a reduction in field-effect passivation for high N_d. Comparing the two X_{TCO}, it can be seen that the dependence on N_d is less pronounced for high X_{TCO}. This can be explained by the fact that the band bending is mostly affected by X_{TCO} and its change affects $\Delta\phi$ directly, whereas the change in work function from $N_d = 1\cdot10^{19}$ to $1\cdot10^{21}$ cm^{-3} is only ~120 meV.
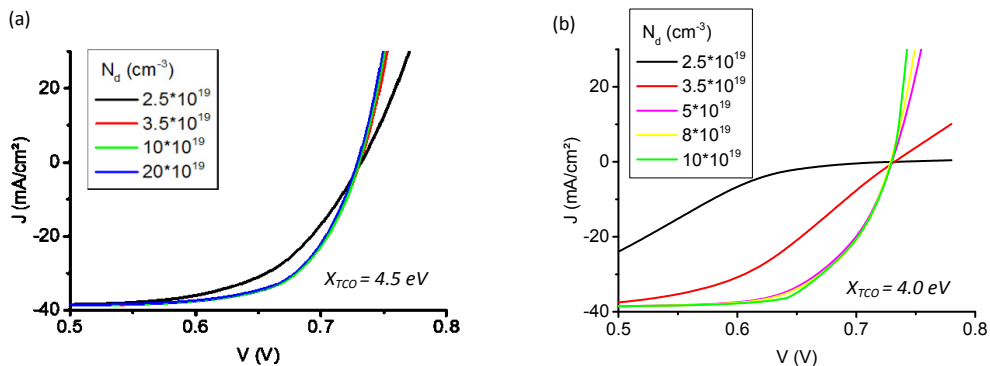

Fig. 6. Simulated light J-V characteristics at high forward bias for electron affinitys of (a) $X_{TCO} = 4.5$ eV and (b) $X_{TCO} = 4.0$ eV and varying N_d.

5. Conclusions and outlook

Solar cells with ITO contact layers with various dopant densities, N_d, have been investigated. The systematic formation of S-shaped J-V characteristics (increased R_{oc}) is observed for ITO contact layers with decreasing doping densities (and presumably increased work function) for $N_d < 2\cdot10^{19}$ cm^{-3}. On the other hand, the negative influence of reduced field passivation on the device performance for very high charge carrier densities is relatively low. These

trends can qualitatively be reproduced using the device simulator *AFORS-HET* when tunneling models are considered, which suggests that inefficient tunneling can lead to the S-shaped J-V characteristics.

Under the assumption that the work function increases with reducing N_d (an assumed constant electron affinity), the presented data indicate that there are two competing mechanisms: (1) a good field effect passivation demands a high work function (low N_d), whereas (2) an efficient tunnel recombination contact demands a low work function (high N_d). This aspect should be considered in the search for an "ideal" TCO contact layer for HIT solar cells.

The best manufactured solar cell had a contact layer with $N_d = 2.3 \cdot 10^{19}$ cm^{-3}. The data indicates that a slight increase in N_d could further improve the contact resistivity. For more meaningful and predictive simulations in the future, a calibration of the model and determination of the many unknown parameters by in-depth characterization and analyses is essential.

Acknowledgements

Appendix A. important model input parameters

Parameter	Thickness (nm)	Electron affinity, X (eV)	Mobility gap (eV)	Dopant density, N_d (cm^{-3}), activation energy (meV)	Defect density (cm^{-3})	Electron (hole) mobility (cm²/Vs)	F_0 (V/cm)	m^* / $m_{electron}$
TCO	80	4.5, 4.8	4	variable	–	40 (20)	–	–
a-Si:H(p)	8	4	1.72	10^{20}, 200	$4 \cdot 10^{20}$	20 (5)	$2 \cdot 10^{5}$	0.012

References

[1] Taguchi M, Yano A, Tohoda S, Matsuyama K, Nakamura Y, Nishiwaki T, Fujita K, Maruyama E, 24.7 % Record Efficiency HIT Solar Cell on Thin Silicon Wafer. IEEE J Photovolt; 2014 4:96.

[2] Lee S-Y, Choi H, Li H, Ji K, Nam S, Choi J, Ahn S-W, Lee H-M, Park B. Analysis of a-Si:H/TCO contact resistance for the Si Heterojunction Back-Contact Solar Cell. Sol En Mat and Sol Cells; 2014 120:412.

[3] Varache R, Kleider JP, Gueunier-Farret ME, Korte L. Silicon Heterojunction Solar Cells: Optimization of Emitter and Contact Properties from Analytical Calculation and Numerical Simulation. Mat Sci and Eng; 2013 9:593.

[4] Zhao L, Zhou CL, Li HL, Diao HW, Wang WJ. Role of the Work Function of Transparent Conductive Oxide on the Performance of Amorphous/Crystalline Silicon Heterojunction Solar Cells Studied by Computer Simulation. Phys Stat Sol A; 2008 205: 1215.

[5] Rached D, Mostefaoui R. Influence of the Front Contact Barrier Height on the Indium Tin Oxide/Hydrogenated p-Doped Amorphous Silicon Heterojunction Solar Cells. Thin Sol Films; 2008 516:5087.

[6] Bivour M, Schröder S, Hermle M. Numerical Analysis of Electrical *TCO*/a-Si:H(p) Contact Properties for Silicon Heterojunction Solar Cells. En Proc; 2013 38:658.

[7] Kanevce A, Metzger WK. The Role of Amorphous Silicon and Tunneling in Heterojunction with Intrinsic Thin Layer (HIT) Solar Cells. J Appl Phys; 2009 105: 094507.

[8] Rößler R, Leendertz C, Korte L, Mingirulli N, Rech B. Impact of the Transparent Conductive Oxide Work Function on Injection-Dependent a-Si:H/c-Si Band Bending and Solar Cell Parameters. J Appl Phys; 2013 113: 144513.

[9] Macco B, Deligiannis D, Smit S, van Swaaij RACMM, Zeman M, Kessels WMM. Influence of Transparent Conductive Oxides on Passivation of a-Si:H/c-Si Heterojunctions as Studied by Atomic Layer Deposited Al-doped ZnO. Semicond Sci and Tech, 2014 29:122001.

[10] Klein A, Körber C, Wachau A, Säuberlich F, Gassenbauer Y, Harvey SP, Proffit DE, Mason TO. Transparent Conducting Oxides for Photovoltaics: Manipulation of Fermi level, Work Function and Energy Band Alignment. Materials; 2010 3: 4892.

[11] Sugiyama K, Ishii H, Ouchi Y, Seki K. Dependence of ITO Work Function on Surface Cleaning Method as Studied by Ultraviolet and X-ray Photoemission Spectroscopies. J Appl Phys; 2000 87:295.

[12] Kim JS, Lägel B, Moons E, Johansson N, Baikie ID, Salaneck WR, Friend RH, Cacialli F. Kelvin Probe and Ultraviolet Photoemission Measurements of Indium Tin Oxide Work Function: a Comparison. Synth Metals; 2000 111: 311.

[13] Mazzarella L, Kirner S, Mews M, Conrad E, Korte L, Stannowski B, Rech B, Schlatmann R. Comparison of TMB and B_2H_6 as Precursors for Emitter Doping in High Efficiency Silicon Hetero Junction Solar Cells. En Proc; 2014 60:123.

[14] Leendertz C, Stangl R, Modelling an a-Si:H/c-Si Solar Cell with AFORS-HET. In: van Sark WGJHM , Korte L, Roca F, editors, Physics and Technology of Amorphous-Crystalline Heterostructure Silicon Solar Cells, Berlin: Springer; 2012. p. 459–482.

[15] Hurkx GAM, Klaassen DBM, Knuvers MPG. A new Recombination Model for Device Simulation Including Tunneling. IEEE Trans Elec Dev; 1992 39:331.

[16] Willemen JA, Zeman M, Metselaar JW. Computer Modelling of Amorphous Silicon Tandem Cells. In: Proc. of 1st WCPC-I, Hawaii; 1994 p. 599–602.

[17] Zeman M, Willemen JA, Vosteen LLA, Tao G, Metselaar JW. Computer Modelling of Current Matching in a-Si:H/a-Si:H Tandem Solar Cells on Textured TCO Substrates. Sol En Mat and Sol Cells; 1997 46:81.

[18] Juska G, Kocka J, Arlauskas K, Jukonis G. Electron Drift Mobility in a-Si:H under Extremely High Electric Field. Sol State Comm; 1990 75:531.

[19] Bivour M, Reichel C, Hermle M, Glunz SW. Improving the a-Si:H(p) Rear Emitter Contact of n-Type Silicon Solar Cells. Sol En Mat and Sol Cells; 2012 106:11.